

ACCEPTED MANUSCRIPT

This is an early electronic version of an as-received manuscript that has been accepted for publication in the Journal of the Serbian Chemical Society but has not yet been subjected to the editing process and publishing procedure applied by the JSCS Editorial Office.

Please cite this article as M. Bigović, I. S. Veljković, J. Petrović, and D. Ž. Veljković, *J. Serb. Chem. Soc.* (2024) <https://doi.org/10.2298/JSC250125013B>

This “raw” version of the manuscript is being provided to the authors and readers for their technical service. It must be stressed that the manuscript still has to be subjected to copyediting, typesetting, English grammar and syntax corrections, professional editing and authors’ review of the galley proof before it is published in its final form. Please note that during these publishing processes, many errors may emerge which could affect the final content of the manuscript and all legal disclaimers applied according to the policies of the Journal.



J. Serb. Chem. Soc. **00(0)** 1-14 (2025)
JSCS-13222

Quantum-chemical study of C–H···O interactions between HTcO₄ and aromatic amino acids

MILJAN BIGOVIĆ¹, IVANA S. VELJKOVIĆ², JELENA PETROVIĆ³ AND DUŠAN Ž. VELJKOVIĆ^{4*}

¹Faculty of Natural Sciences and Mathematics, University of Montenegro, Podgorica, Montenegro, ²University of Belgrade – Institute for Chemistry, Technology and Metallurgy – National Institute of the Republic of Serbia, Belgrade, Serbia, ³Center for Nuclear Medicine with PET, University Clinical Center of Serbia, Belgrade, Serbia; ⁴Faculty of Medicine, University of Belgrade, Belgrade, Serbia, and ⁴University of Belgrade - Faculty of Chemistry, Belgrade, Serbia.

(Received 25 January; revised 4 February; accepted 7 February 2025)

Abstract: This study investigates C–H···O interactions between HTcO₄ and aromatic amino acids (phenylalanine, tyrosine, and tryptophan) through quantum-chemical calculations. The interaction energies calculations were combined with the analysis of Molecular Electrostatic Potentials (MEP) to understand the nature of these interactions. The strongest interaction was observed for the HTcO₄–tryptophan with an energy minimum of -9.53 kJ/mol at a distance of 2.1 Å. Phenylalanine showed a similarly strong interaction, with a minimum of -9.49 kJ/mol, while tyrosine exhibited the weakest interaction, with a minimum of -8.61 kJ/mol. Electrostatic potential maps confirmed the electrostatic nature of the C–H···O interactions, highlighting the role of the oxygen atoms in acting as hydrogen bond acceptors. These findings suggest that the position of the hydrogen atoms relative to the substituents on the aromatic ring influences the strength of the interactions. The results presented here could be of great importance for the recognition of new, overlooked noncovalent contacts between pertechnetetic acid and amino acid fragments and a better understanding of the stability of pertechnetate-peptide complexes.

Keywords: hydrogen bond; pertechnetetic acid; *ab initio* calculations.

INTRODUCTION

Technetium (Tc), particularly its radionuclide isotope technetium-99m (Tc-99m), is widely used in medicine primarily for diagnostic purposes in nuclear imaging.¹ One of the most common applications of Tc-99m and its compounds like pertechnetate anion (TcO₄⁻) is in detecting and characterizing tumors through

* Corresponding author. E-mail: vdusan@chem.bg.ac.rs
<https://doi.org/10.2298/JSC250125013B>

imaging techniques such as single photon emission computed tomography.^{2,3} Due to its advantageous characteristics, including a short half-life, a low radiation dose to patients, and the capability to be integrated into various compounds that target specific organs or tissues, Tc-99m serves as an excellent agent for diagnostic imaging. It provides crucial information about organ function and facilitates the early detection of diseases such as cancer, heart conditions, and bone disorders. Also, its rapid excretion from the body helps to minimize potential toxic effects. In addition to its diagnostic capabilities, Tc-99m plays a role in therapeutic applications, particularly in targeted radiotherapy. The ability to label peptides and other biomolecules with Tc-99m enhances their utility in targeting malignant tissues, thereby improving the efficacy of treatment while minimizing damage to surrounding healthy tissues.⁴ Beyond its radiopharmaceutical applications, TcO_4^- exhibits intriguing noncovalent interactions in metal complexes and biological systems. As a ligand, TcO_4^- anion forms different noncovalent interactions in metal complexes, including $\text{Tc}\cdots\text{O}$ and $\text{Tc}-\text{O}\cdots\text{H}-\text{O}$ hydrogen bonds.⁵ These contacts are essential for the formation of 1D and 2D supramolecular assemblies, highlighting the multifaceted role of TcO_4^- in both medical and structural chemistry. Quantum chemical calculations at the PBE0-D4/def2-TZVP level determined that the interaction energies for dimers involving $\text{Tc}\cdots\text{O}$ contacts range from -6.57 to -10.13 kJ/mol, indicating relatively modest interaction strengths.

On the other hand, noncovalent interactions of Tc-99m and its compounds within biological systems, particularly with biomolecules, remain less explored and mainly focused on Tc-binding in labeled peptides.⁶⁻⁹ Understanding these interactions is crucial for elucidating potential reaction pathways and binding mechanisms. Among these, the study of $\text{C}-\text{H}\cdots\text{O}$ hydrogen bonding offers valuable insight, especially in systems involving aromatic amino acids. This type of interaction, often overlooked compared to stronger hydrogen bonds, plays a significant role in stabilizing molecular assemblies and influencing biological processes. Previous analysis of protein crystal structures showed that approximately 25% of all noncovalent interactions in proteins are $\text{C}-\text{H}\cdots\text{O}$ interactions.¹⁰

$\text{C}-\text{H}\cdots\text{O}$ interactions involving aromatic $\text{C}-\text{H}$ donors have been investigated in various systems.¹¹⁻¹³ Findings from crystal data analysis indicate that aromatic $\text{C}-\text{H}\cdots\text{O}$ interactions do not strongly favor linear geometries. MP2/cc-pVTZ calculations report stabilization energies for linear interactions of benzene with water, methanol, and acetone as -5.36, -6.15, and -6.07 kJ/mol, respectively.¹¹ The study of $\text{C}-\text{H}\cdots\text{O}$ interactions between nucleic bases and water reveals that bifurcated interactions are significantly stronger than linear contacts.¹³ This study found that the strongest linear interaction occurs with uracil (-15.02 kJ/mol), followed by other bases, all remaining above -8.37 kJ/mol except for adenine. However, in the case of aromatic amino acids in proteins, analysis of

crystallographic data showed that bifurcated interactions represent only 3% of all C–H···O contacts.¹⁴ Analysis of electrostatic potential maps of aromatic amino acids (phenylalanine, tyrosine, and tryptophan) within the same study showed that most positive regions in the area of C–H fragments in these amino acids are positioned in the region of H atom, along the C–H direction.

The main goal of this study is to investigate the potential for hydrogen bonding between aromatic amino acids and pertechnetate compounds. Understanding the ability of pertechnetates to interact with aromatic amino acids residues through C–H···O contacts could provide valuable insights into its biochemical reactivity and implications for biological systems.

EXPERIMENTAL

Energies of C–H···O interactions were calculated for model systems containing technetium (VII) oxoacid (pertechnetetic acid, HTcO₄) and aromatic amino acids—phenylalanine, tyrosine, and tryptophan. High-level ab initio calculations were performed using the Gaussian 09 software.¹⁵ Geometry optimizations of monomers employed the MP2 method¹⁶ with the def2-TZVP basis set¹⁷ for HTcO₄ and the cc-pVTZ basis set¹⁸ for the amino acids (Tables S1 – S4). The basis sets for HTcO₄ and amino acid molecules were chosen based on recommendations from previous studies on the interaction energies of these molecules.^{5, 14} Vibrational frequency calculations were performed for all optimized geometries (Figure 1) to ensure that they correspond to true minima on the potential energy surface, confirmed by the absence of imaginary frequencies.

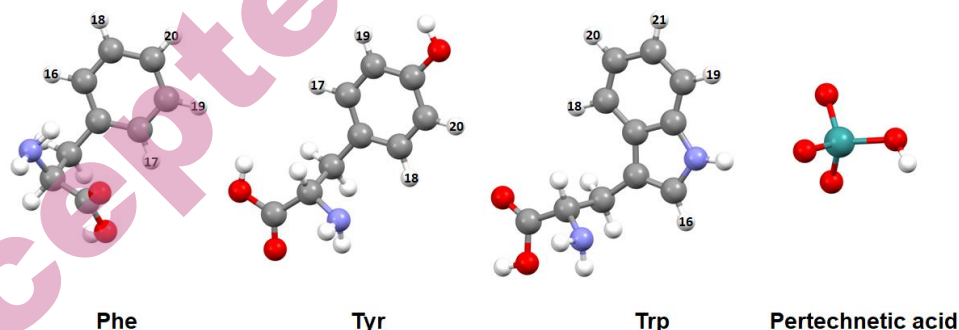


Fig 1. Optimized geometries of phenylalanine (Phe), tyrosine (Tyr), tryptophan (Trp), and pertechnetetic acid. Hydrogen atoms in the aromatic amino acids are labeled to denote potential interaction sites as C–H donors.

Interaction energies were calculated at the MP2/def2-TZVP level of theory with BSSE corrections via the counterpoise method¹⁹ to ensure accuracy. An electrostatic potential (ESP) map was generated using the gOpenMol software²⁰ to visualize charge distributions and identify interaction sites. To further investigate the nature of the strongest interaction, Mulliken charges were calculated for the HTcO₄ species to gain insight into the electron distribution and the potential electrostatic interactions in the system.

Model systems comprising HTcO₄ and three different aromatic amino acid were constructed, where the Tc–O–H plane plane is positioned perpendicular to the aromatic ring

plane of each amino acid (Figure 2) to avoid simultaneous interactions with other parts of aromatic fragment.

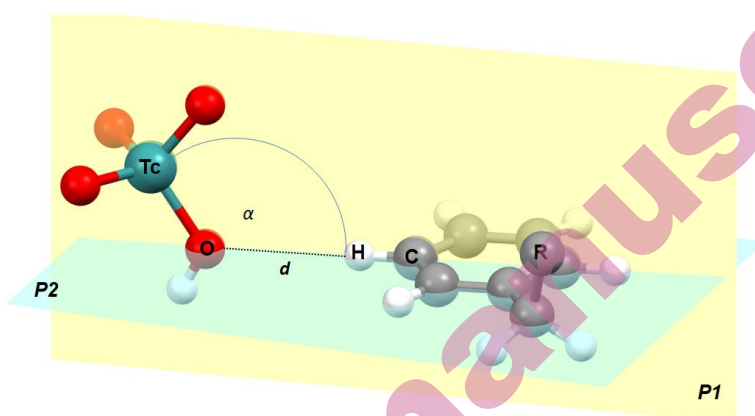


Fig 2. General scheme of the model systems showing interactions between pertechnetetic acid (HTcO_4) and the aromatic rings of phenylalanine, tyrosine, and tryptophan. The plane **P1** contains the Tc–O–H atoms of HTcO_4 , while plane **P2** is the average plane of the aromatic ring. The angle α represents the angle formed by the Tc–O–H atoms. The distance d denotes the distance between the oxygen atom of HTcO_4 and the hydrogen atom of the C–H donor.

The angle (α) formed between technetium, oxygen, and hydrogen atoms was set at 120° , since earlier study of C–H \cdots O interactions showed that this geometry is most common in the case of C–H \cdots O interactions between C–H fragment from aromatic hydrogen donor and molecules of R–O–H type.¹¹ The distance (d) between the oxygen atom of HTcO_4 and the hydrogen from the C–H donor was systematically varied from 2.0 to 2.9 Å. In the structures of phenylalanine, tyrosine, and tryptophan, multiple C–H \cdots O interactions are possible due to the presence of different hydrogen atoms. Phenylalanine can form three distinct C–H \cdots O interactions, tyrosine two, and tryptophan five. These interactions are determined by the position of hydrogen atoms within the aromatic systems of the amino acids, each offering unique interaction sites. Different interactions were systematically analyzed to understand the role of these hydrogen donors in stabilizing complexes with pertechnetetic acid. The Cambridge Structural Database (CSD)²¹ was searched for all crystal structures containing X–H \cdots O–Tc fragment containing tetracoordinate Tc atom. The H \cdots O distance was set to be less than 2.9 Å, and the C–H \cdots O angle values were set to be between 110° and 180° , in accordance with previously established criteria for this type of interactions.¹⁴

RESULTS AND DISCUSSION

Interaction energy analysis in the HTcO_4 –Phenylalanine model systems

As mentioned in the Methodology section, the model system involving HTcO_4 and phenylalanine includes three distinct hydrogen atoms, labeled as H16, H18, and H20, as shown in Figure 1. The interaction energies between pertechnetetic acid and these specific hydrogen atoms were analyzed in detail to investigate their contribution to the overall stability of the system. In the HTcO_4 –Phe system, the

strongest interaction was observed between the oxygen atom of HTcO₄ and the H16 atom of phenylalanine at a distance of 2.3 Å (Figure 3).

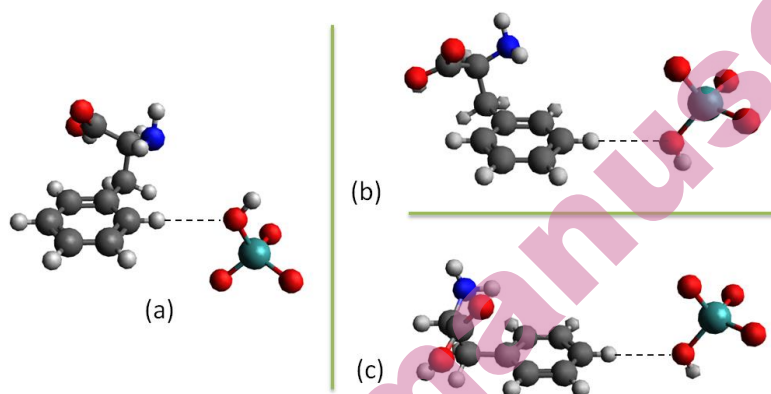


Fig 3. Studied C–H···O interaction sites in the HTcO₄–Phe model system: (a) interaction with the hydrogen atom labeled H16, (b) interaction with the hydrogen atom H18, and (c) interaction with the hydrogen atom H20.

This interaction exhibited an energy minimum of -9.50 kJ/mol (Figure 4), indicating a relatively strong C–H···O hydrogen bond. In comparison, the interaction energy of linear C–H···O interaction between water and benzene molecule was calculated to be -5.36 kJ/mol.¹¹ For the H18 interaction, the energy minimum was observed at slightly larger distances of 2.4 Å and 2.5 Å, with an interaction energy of -6.19 kJ/mol. Although weaker than the interaction with H16, it remains significant. Similarly, the interaction involving the H20 atom occurred at the same distances of 2.4 Å and 2.5 Å. However, the energy minimum was -5.89 kJ/mol, making it the weakest among the three model systems.

When comparing the interaction energies, the HTcO₄–H16 system demonstrated the strongest interaction, followed by the interactions with H18 and H20. This suggests that the position of the hydrogen atom in the phenylalanine structure critically influences the strength of the C–H···O hydrogen bond. The interaction energies for H18 and H20 are similar, likely due to the comparable spatial positions of these hydrogen atoms relative to the aromatic ring substituent, which does not significantly hinder or enhance their interaction with the HTcO₄ molecule (Figure 3). In contrast, the stronger interaction with H16 can be attributed to the proximity of the substituent on the aromatic ring to both H16 and the interacting HTcO₄ molecule, which facilitates a more favorable environment for the C–H···O hydrogen bond formation.

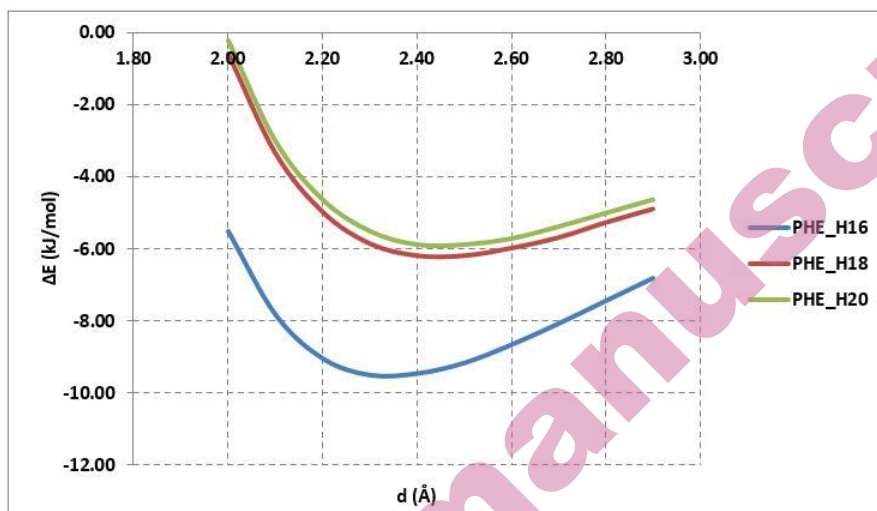


Fig 4. Potential energy curves for the HTcO₄-Phe model system, showing the interactions with hydrogen atoms H16, H18, and H20 calculated at MP2/def2-TZVP level of theory.

Interaction analysis in the HTcO₄-Tyrosine model system

The HTcO₄-tyrosine system was analyzed by examining the interactions involving hydrogen atoms H17 and H19 (Figure 5).

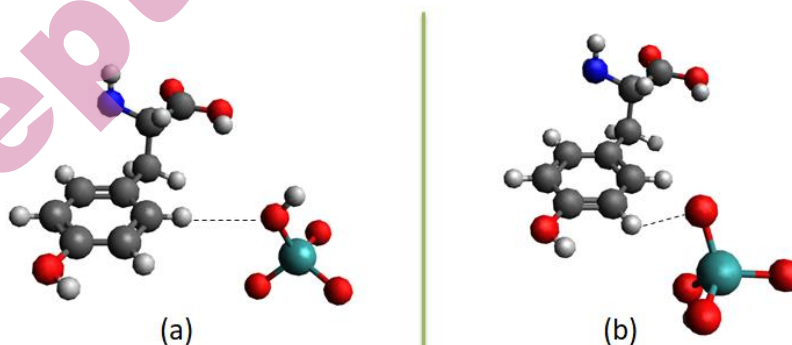


Fig 5. Investigated C-H...O interaction sites in the model system of HTcO₄ and tyrosine: (a) interaction with hydrogen atom denoted as H17, and (b) interaction with hydrogen atom H19.

The interaction with H19 exhibited the strongest interaction energy, with a minimum of -8.61 kJ/mol at a distance of 2.4 Å (Figure 6).

This suggests a relatively strong C-H...O hydrogen bond. In comparison, the interaction with H17 was slightly weaker, showing an energy minimum of -8.45 kJ/mol at a slightly longer distance of 2.5 Å.

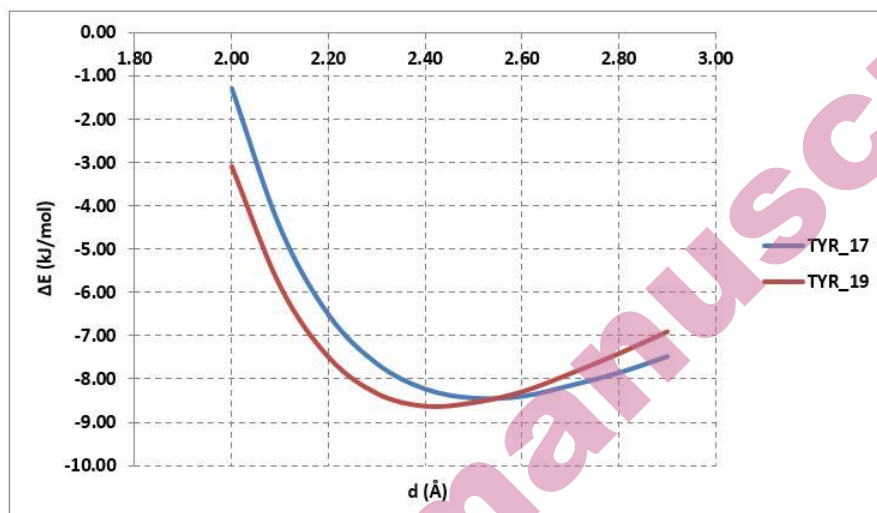


Fig 6. Potential energy curves for the HTcO₄-Tyr model system, showing the interactions with hydrogen atoms H17 and H19 calculated at MP2/def2-TZVP level of theory.

Interaction analysis in the HTcO₄-Tryptophan model system

The HTcO₄-tryptophan system reveals a diverse range of interaction strengths and distances, influenced by the positions of hydrogen atoms within the tryptophan structure (Figure 7). The strongest interaction was observed between HTcO₄ and H18, with an interaction energy minimum of -9.54 kJ/mol occurring at the shortest distance of 2.1 Å (Figure 8). This configuration demonstrates a highly stable hydrogen bond, attributable to the proximity of H18 to the oxygen atom of HTcO₄ and its favorable spatial arrangement.

The interaction with H16, though slightly weaker than H18, also represents a significant stabilization with an energy minimum of -9.41 kJ/mol. The distance for this interaction ranged between 2.3 Å and 2.4 Å, slightly longer than for H18. This suggests that while H16 is capable of forming a strong C-H···O bond, its geometric positioning relative to HTcO₄ is marginally less optimal than H18.

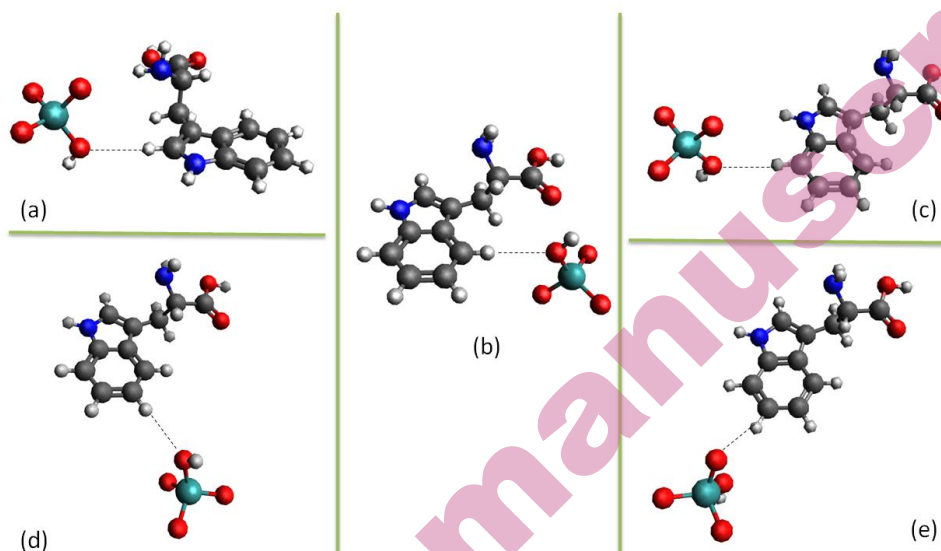


Fig 7. C–H···O interaction sites identified in the model system of HTcO₄ and tryptophan: (a) interaction with the hydrogen atom H16, (b) interaction with H18, (c) interaction with H19, (d) interaction with H20, and (e) interaction with H21.

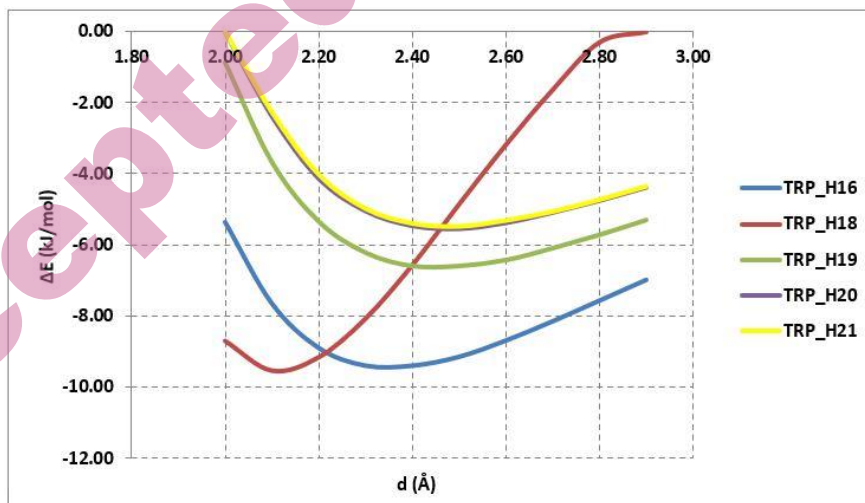


Fig 8. Potential energy curves for the HTcO₄–Trp model system, showing the interactions with hydrogen atoms H16, H18, H19, H20, H21. calculated at MP2/def2-TZVP level of theory.

Moving to interactions with H19, H20, and H21, a progressive weakening of the interaction energy was noted. For H19, the energy minimum was measured at -6.60 kJ/mol at distances of 2.4 Å and 2.5 Å. Although the distance is comparable

to that observed for H16, the interaction strength is notably lower, indicating that the electronic environment and substituent effects around H19 influence its bonding capacity negatively. The interactions with H20 and H21 were the weakest, with energy minima of -5.56 kJ/mol and -5.48 kJ/mol, respectively, occurring at a distance of 2.5 Å. These interactions, while still indicative of C–H···O hydrogen bonding, are substantially weaker, likely because the substituent on the aromatic structure of tryptophan is positioned further away from the interacting HTcO₄ molecule, reducing its capacity to enhance the interaction through proximity effects. The observed hierarchy in interaction strengths (H18 > H16 > H19 > H20 > H21) underscores the critical role of hydrogen atom positioning and the surrounding molecular environment in determining the strength of the hydrogen bond. The exceptionally strong interaction with H18 and its shorter distance suggests a synergistic interplay of steric and electronic factors. On the other hand, the interactions with H20 and H21 reflect weaker hydrogen bonding, potentially constrained by the aromatic system's substituent effects and the spatial orientation of HTcO₄.

In comparing the strongest interactions across the three model systems (HTcO₄–phenylalanine, HTcO₄–tryptophan, and HTcO₄–tyrosine), the interaction energies varied, reflecting the differences in atomic positions and the nature of the interactions. Among all systems, the strongest interaction was observed in the HTcO₄–tryptophan system, with an energy minimum of -9.53 kJ/mol at a distance of 2.1 Å. This was followed by the HTcO₄–phenylalanine system, which displayed an energy minimum of -9.49 kJ/mol at 2.3 Å. The weakest interaction was found in the HTcO₄–tyrosine system, with a minimum energy of -8.61 kJ/mol at 2.4 Å. These results demonstrate that the position of the hydrogen atom and the spatial arrangement of the substituents in each amino acid significantly influence the strength of the C–H···O hydrogen bonding interactions.

Molecular Electrostatic Potential Surfaces (MEPS)

To further understand the strengths of the interactions, we calculated the electrostatic potential map (Figure 9) for pertechnetetic acid. Since C–H···O interactions are largely governed by electrostatic forces, the map was analyzed to reveal key regions of negative and positive potentials.

Blue color represents regions of negative potential, which are located around the oxygen atoms, indicating their role as hydrogen bond acceptors. In contrast, red represents positive potential, which is observed around the hydrogen and metal atoms. This distribution supports the concept that the oxygen atoms are potential hydrogen bond acceptors in these interactions.

To quantitatively describe the distribution of charges, Mulliken population analysis was performed and calculated Mulliken charges are given in Figure 10.

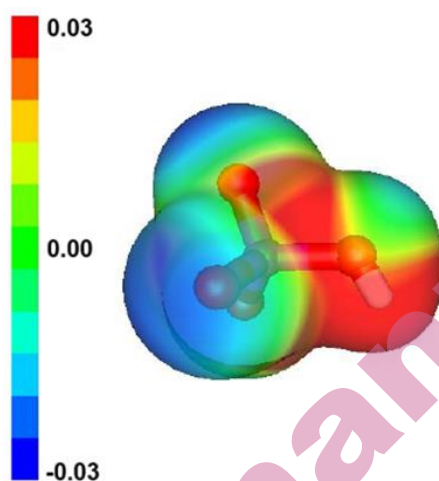


Fig 9. Electrostatic potential (ESP) map of pertechnetetic acid (HTcO_4) with the contour map.

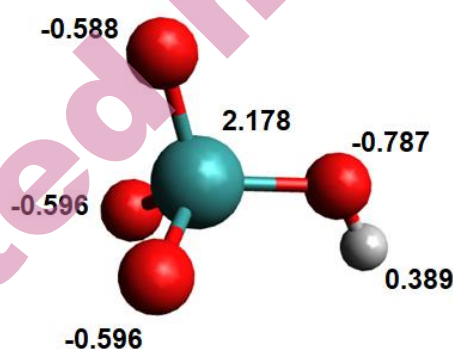


Fig 10. Mulliken atomic charges calculated for HTcO_4 molecule. The oxygen atom bonded to both Tc and H exhibits a significantly more negative charge (-0.787), making it the primary site for strong $\text{C-H}\cdots\text{O}$ interactions with aromatic C-H donors.

Distribution of Mulliken charges shows that oxygen atoms connected only to the Tc atom have similar values of Mulliken charges (from -0.596 to -0.588), while oxygen atom connected to both Tc and H atom has significantly more negative value of Mulliken charge (-0.787), due to the polarization effects resulting from its dual bonding to Tc and H. These results confirm that the interacting oxygen atom is indeed the most likely to form the strongest $\text{C-H}\cdots\text{O}$ interaction with aromatic C-H donors from studied amino acids.

Analysis of crystal structures

The Cambridge Structural Database was searched for all crystal structures containing $\text{X-H}\cdots\text{O-Tc}$ interactions involving tetracoordinated Tc species. Four crystal structures met the criteria used in the CSD search (KACWAO, KACWES,

WAHQIG, YAKZUF). A fragment of the KACWAO crystal structure is shown in Figure 11.

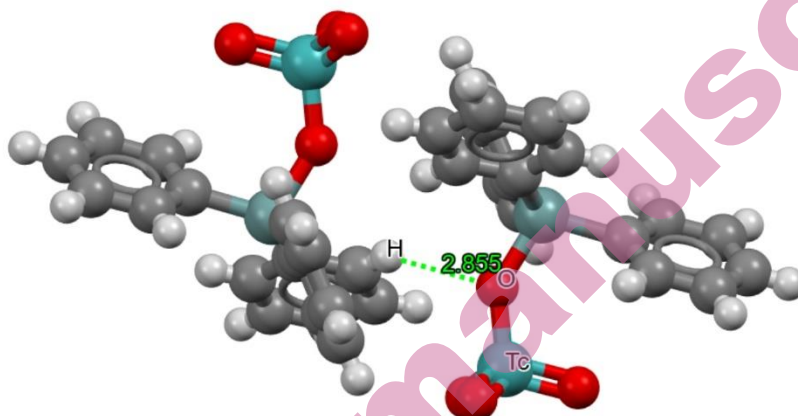


Fig 11. C–H···O–Tc interaction identified in a fragment of the KACWAO crystal structure.

In this crystal structure, a C–H···O interaction involving an aromatic C–H donor and an oxygen atom bonded to Tc was detected. The distance between the interacting O and H atoms is less than 2.9 Å, which is consistent with expected values for C–H···O contacts.¹⁰ The C–H···O angle is 145.24°, falling within the typical range for such interactions (110–180°).¹⁰ A similar interaction was observed in the other extracted crystal structures. The analysis of geometric parameters in these structures confirms that C–H···O interactions between aromatic C–H donors and the O–Tc fragment indeed occur in experimentally determined crystal structures.

CONCLUSION

The goal of this study was to investigate and characterize C–H···O interactions between pertechnetate acid (HTcO₄) molecule and aromatic amino acids: phenylalanine, tyrosine, and tryptophan. Interaction energies, calculated at the MP2/def2-TZVP level, confirmed strong linear C–H···O interactions, with the strongest observed for the HTcO₄–tryptophan system (-9.53 kJ/mol at 2.1 Å). Very strong interactions were also observed in HTcO₄–phenylalanine (-9.49 kJ/mol at 2.3 Å) and HTcO₄–tyrosine (-8.61 kJ/mol at 2.4 Å) systems. Compared to similar systems involving nucleobases, and aromatic molecules, the interactions between HTcO₄ and aromatic amino acids as C–H donors are among the strongest known. The molecular electrostatic potential analysis revealed that there are areas of strong negative potential around all oxygen atoms in the HTcO₄ molecule. Mulliken population analysis showed that the most negative oxygen atom is the one in the O–H fragment of HTcO₄, making it the most likely candidate for hydrogen bond

acceptors in C–H···O interactions. The analysis of geometric parameters confirms that C–H···O interactions between aromatic C–H donors and the O–Tc fragment are present in experimentally determined crystal structures. These findings highlight the role of C–H···O contacts in systems containing pertechnetate species and aromatic amino acids. Also, presented results can be significant for the recognition of often-overlooked weak hydrogen bonds in protein- HTcO_4 adducts.

SUPPLEMENTARY MATERIAL

Additional data are available electronically at the pages of journal website: <https://www.shd-pub.org.rs/index.php/JSCS/article/view/13222>, or from the corresponding author on request.

Acknowledgements: This research has been supported by the Ministry of Science, Technological Development and Innovation of Republic of Serbia (Contract numbers: 451-03-66/2024-03/200026 and 451-03-66/2024-03/200168). The authors would like to thank Zorana Zeković for her assistance with interaction energy calculations

ИЗВОД

КВАНТНОХЕМИЈСКО ПРОУЧАВАЊЕ C–H···O ИНТЕРАКЦИЈА ИЗМЕЂУ HTcO_4 И АРОМАТИЧНИХ АМИНОКИСЕЛИНА

МИЉАН БИГОВИЋ¹, ИВАНА С. ВЕЉКОВИЋ², ЈЕЛЕНА ПЕТРОВИЋ³ И ДУШАН Ж. ВЕЉКОВИЋ^{4*}

¹Природно математички факултет Универзитета Црне Горе, Подгорица, Црна Гора, ²Универзитет у Београду – Институт за хемију, технологију и металургију – Институт од Националног значаја за Републику Србију, Београд, Србија, ³Центар за нуклеарну медицину са позитронском емисионом томографијом, Универзитетски клинички центар Србије; Универзитет у Београду, Медицински факултет, Београд, Србија, и ⁴Универзитет у Београду – Хемијски факултет, Београд, Србија.

У овом раду су проучаване C–H···O интеракције између HTcO_4 и ароматичних аминокиселина (фенилаланин, тирозин и триптофан) коришћењем квантнохемијских прорачуна. Резултати прорачуна енергије интеракција су комбиновани са анализом молекулских електростатичких потенцијала (МЕП) ради бољег разумевања природе ових интеракција. Најјача интеракција је израчуната у систему HTcO_4 –триптофан са минимумом од $-9,53 \text{ kJ/mol}$ на растојању од $2,1 \text{ \AA}$. Фенилаланин је показао сличну јачину интеракције ($-9,49 \text{ kJ/mol}$), док тирозин има најслабију интеракцију ($-8,61 \text{ kJ/mol}$). Анализа мале електростатичког потенцијал је потврдила електростатичку природу C–H···O интеракција, наглашавајући улогу атома кисеоника као акцептора водоника у водоничним везама. Ови резултати пружају значајан увид у улогу C–H···O интеракција у молекулском препознавању и дизајну функционалних материјала са пертехнетатским јединицама. Добијени резултати указују да положај атома водоника у односу на супституенте на ароматичном прстену утичу на енергију ових интеракција. Ови резултати могу бити од великог значаја за препознавање нових нековалентних контаката између пертехнетатских киселина и фрагмената аминокиселина, као и за боље разумевање стабилности комплекса пертехнетата и пептида.

(Примљено 25. јануара; ревидирано 4. фебруара; прихваћено 7. фебруара 2025.)

REFERENCES

1. D. Papagiannopoulou, *J. Label. Compd. Radiopharm.* **60** (2017) 502 (<https://doi.org/10.1002/jlcr.3531>).
2. J. G. O'Connell-Danes, B. T. Ngwenya, C. A. Morrison, J. B. Love, *Angew. Chem. Int. Ed.* **63** (2024) e202409834 (<https://doi.org/10.1002/anie.202409834>).
3. S. M. Rathmann, Z. Ahmad, S. Slikboer, H. A. Bilton, D. P. Snider, J. F. Valliant, *The Radiopharmaceutical Chemistry of Technetium-99m*. in *Radiopharmaceutical Chemistry*, J. Lewis, A. Windhorst, B. Zeglis, Eds., Springer, Cham., 2019, p. 311 (https://doi.org/10.1007/978-3-319-98947-1_18).
4. J. Chen, Z. Cheng, Y. Miao, S. S. Jurisson, T. P. Quinn, *Cancer* **94** (2002) 1196 (<https://doi.org/10.1002/cncr.10284>).
5. D. Grödler, S. Burguera, A. Frontera, E. Strub, *Chem. Eur. J.* **30** (2024) e202400100 (<https://doi.org/10.1002/chem.202400100>).
6. R. Waibel, R. Alberto, J. Willuda, R. Finner, R. Schibli, A. Stichelberger, A. Egli, U. Abram, J.-P. Mach, A. Plückthun, P. A. Schubiger, *Nat. Biotechnol.* **17** (1999) 897 (<https://doi.org/10.1038/12890>).
7. M. Bartholomä, J. Valliant, K. P. Maresca, J. Babich, J. Zubieta, *Chem. Commun.* **5** (2009) 493 (<https://doi.org/10.1039/B814903H>).
8. M. B.-U. Surfraz, R. King, S. J. Mather, S. Biagini, P. J. Blower, *J. Inorg. Biochem.* **103** (2009) 971 (<https://doi.org/10.1016/j.jinorgbio.2009.04.007>).
9. D. Hernández-Valdés, R. Alberto, U. Jáuregui-Haza, *RSC Adv.* **6** (2016) 107127 (<https://doi.org/10.1039/C6RA23142J>).
10. K. Manikandan, S. Ramakumar, *Proteins* **56** (2004) 768 (<https://doi.org/10.1002/prot.20152>).
11. D. Ž. Veljković, G. V. Janjić, S. D. Zarić, *CrystEngComm* **13** (2011) 5005 (<https://doi.org/10.1039/C1CE05065F>).
12. D. Ž. Veljković, *J. Mol. Graph. Model.* **80** (2018) 121 (<https://doi.org/10.1016/j.jmgm.2017.12.014>).
13. D. Ž. Veljković, V. B. Medaković, J. M. Andrić, S. D. Zarić, *CrystEngComm* **16** (2014) 10089 (<https://doi.org/10.1039/C4CE00595C>).
14. J. Lj. Dragelj, I. M. Stanković, D. M. Božinovski, T. Meyer, D. Ž. Veljković, V. B. Medaković, E.-W. Knapp, Snežana D. Zarić, *Cryst. Growth Des.* **16** (2016) 1948 (<https://doi.org/10.1021/acs.cgd.5b01543>).
15. M. J. Frisch, G. W. Trucks, H. B. Schlegel, G. E. Scuseria, M. A. Robb, J. R. Cheeseman, G. Scalmani, V. Barone, B. Mennucci, G. A. Petersson, H. Nakatsuji, M. Caricato, X. Li, H. P. Hratchian, A. F. Izmaylov, J. Bloino, G. Zheng, J. L. Sonnenberg, M. Hada, M. Ehara, K. Toyota, R. Fukuda, J. Hasegawa, M. Ishida, T. Nakajima, Y. Honda, O. Kitao, H. Nakai, T. Vreven, J. A. Montgomery Jr., J. E. Peralta, F. Ogliaro, M. Bearpark, J. J. Heyd, E. Brothers, K. N. Kudin, V. N. Staroverov, R. Kobayashi, J. Normand, K. Raghavachari, A. Rendell, J. C. Burant, S. S. Iyengar, J. Tomasi, M. Cossi, N. Rega, J. M. Millam, M. Klene, C. Adamo, R. Cammi, J. W. Ochterski, R. L. Martin, K. Morokuma, V. G. Zakrzewski, G. A. Voth, P. Salvador, J. J. Dannenberg, S. Dapprich, A. D. Daniels, O. Farkas, J. B. Foresman, J. V. Ortiz, J. Cioslowski and D. J. Fox, Gaussian 09, Revision D.01, Gaussian, Inc., Wallingford CT, 2013.
16. C. Moller, M. S. Plesset, *Phys. Rev.* **46** (1934) 618 (<https://doi.org/10.1103/PhysRev.46.618>).

17. F. Weigend, *Phys. Chem. Chem. Phys.* **8** (2006) 1057 (<https://doi.org/10.1039/B515623H>)
18. T. H. Dunning Jr., *J. Chem. Phys.* **90** (1989) 1007 (<https://doi.org/10.1063/1.456153>).
19. S. F. Boys, F. Bernardi, *Mol. Phys.* **19** (1970) 553 (<https://doi.org/10.1080/00268977000101561>).
20. L. Laaksonen, *J. Mol. Graphics* **10** (1992) 33 ([https://doi.org/10.1016/0263-7855\(92\)80007-Z](https://doi.org/10.1016/0263-7855(92)80007-Z)).
21. C. R. Groom, I. J. Bruno, M. P. Lightfoot, S. C. Ward, *Acta Cryst.* **B72** (2016) 171 (<https://doi.org/10.1107/S2052520616003954>).

Accepted manuscript